Structural stability of the PsbQ protein of higher plant photosystem II†

Mónica Balsera[‡#], Margarita Menéndez[§], José L. Sáiz[§], Javier de las Rivas[‡], José M. Andreu[‖], and Juan B. Arellano[‡*]

[‡] Instituto de Recursos Naturales y Agrobiología (CSIC), Cordel de Merinas 52, 37008 Salamanca; [§] Instituto de Química-Física Rocasolano, Serrano 113, 28006 Madrid; [‖] Centro de Investigaciones Biológicas, Ramiro Maetzu 9, 28040 Madrid, Spain.

[#]current address: Servicio de Medicina y Cirugía Experimental, Hospital General Universitario Gregorio Marañón, Madrid, Spain.

***Corresponding author:** Juan B. Arellano. Phone: +34-923-219606 (Ext. 207). Fax: +34-923-219609. E-mail: jarellano@usal.es

Running title: PsbQ structural stability analysis

---

†This work was funded by the Spanish Ministry of Science and Technology (project references PB1998-0480 and AGL2003-0045). M. Balsera holds a fellowship from the Spanish Ministry of Science and Technology.

Abbreviations: CD, circular dichroism; DSC, differential scanning calorimetry; NPQ, non photochemical quenching; OEC, oxygen-evolving complex; PSII, photosystem II; 3D, three-dimensional; T_m, transition temperature; ΔH_D, calorimetric enthalpy change; ΔH_D^{vH}, van't Hoff enthalpy change, ΔCp_D, denaturation heat capacity change; $[\text{GdnHCl}]_{1/2}$, concentration of GdnHCl giving half denaturation.

ABSTRACT

We have characterized the stability and folding behavior of the isolated extrinsic PsbQ protein of photosystem II (PSII) from a higher plant, *Spinacia oleracea*, using intrinsic protein fluorescence emission and near- and far-UV circular dichroism (CD) spectroscopy in combination with differential scanning calorimetry (DSC). Experimental results reveal that both chemical denaturation using guanidine hydrochloride (GdnHCl) and thermal unfolding of PsbQ proceed as a two-state reversible process. The denaturation free energy changes (ΔG_D) at 20 ^{o}C extrapolated from GdnHCl (4.0±0.6 kcal·mol^{-1}) or thermal unfolding (4.4±0.8 kcal·mol^{-1}) are very close. Moreover, the far-UV CD spectra of the denatured PsbQ registered at 90 ºC in the absence and in the presence of 6.0 M GdnHCl superimpose, letting us conclude that both denatured states of PsbQ are structurally and energetically similar. The thermal unfolding of PsbQ has been also characterized by CD and DSC over a wide pH range. The stability of PsbQ is maximum at pH comprised between 5−8, being wider than the optimal pH for oxygen evolution in the lumen of thylakoid membranes. In addition, no significant structural changes were detected in PsbQ between 50 and 55 ºC in the pH range of 3−8, suggesting that PsbQ behaves as a soluble and stable particle in the lumen when detaches from PSII under physiological stress conditions such as high temperature (45−50 ºC) or low pH (<5.0). Sedimentation experiments showed that, in solution at 20 ºC, PsbQ protein is a monomer with an elongated shape.

The high-energy biochemical reaction of water oxidation takes place in the oxygen-evolving complex (OEC) of Photosystem II (PSII) of oxy-photoautotrophs. It is catalyzed by means of a light-dependent five-step process, the so-called Kok cycle, which occurs at the luminal side of the thylakoid-bound PSII (for review see *1, 2, 3*). The bioinorganic OEC consists of a cluster of four redox active Mn ions and of non-active redox cofactors, Ca^{2+}, Cl^{-} and HCO_3^{-}. The structure of the PSII multienzymatic complex, which consists of about twenty-five intrinsic and extrinsic proteins denoted as PsbA–Z, has been determined by X-ray crystallography in two species of cyanobacteria at 3.8 Å (*4*), 3.7 Å (*5*) and 3.5 Å (*6*). In the 3D structure of the PSII complex, the arrangement of the Mn cluster is shown to be sandwiched between the luminal-facing, high molecular weight proteins of the PSII core (PsbA, PsbB, PsbC and PsbD) and the three luminal extrinsic proteins PsbO, PsbV and PsbU. The recent refined structure of cyanobacterial PSII at 3.5 Å points out that only side chains of PsbA and PsbC bind the four Mn and, possibly, Ca^{2+} (*6*). On comparing the composition, structure and function of the PSII complex among all the oxy-photoautotrophs (*i.e.* the prokaryotic cyanobacteria and green oxy-photobacteria, and the eukaryotic non-green algae, green algae and higher plants), it can be seen that the intrinsic proteins and cofactors of the complex are highly conserved (*7*). In contrast, the extrinsic proteins are different in number, composition or even structure depending on the nature of the oxy-photoautotroph (*8, 9*), but nevertheless their overall function remains still the same. Variations in the extrinsic protein composition from prokaryotic to eukaryotic oxy-photoautotrophs seem to be due to evolutionary reasons. However, there is not yet a clear picture of why.

In particular, PsbO, PsbP and PsbQ are the luminal extrinsic proteins of PSII in higher plants and green algae. Among all the extrinsic proteins of PSII, PsbO is the only orthologous protein in all oxy-photoautotrophs. The loss of PsbO from PSII results in the slow release of the Mn cluster, so it has also been specifically called the manganese stabilizing protein (*10*). PsbP and PsbQ, as PsbU and PsbV, optimize the Ca^{2+} and Cl^{-} environment in the OEC (*11*, *12*) and also protect the Mn cluster from exogenous reductants (*13*). Sequence homology searching has

retrieved some genes from cyanobacteria and green oxy-photobacteria with certain homology to those encoding for PsbP and PsbQ in higher plants (*9*). Recently, PsbP-like and PsbQ-like proteins showing sequence similarity to PsbP and PsbQ have proven experimentally in cyanobacterial PSII preparations (*14, 15*) and so has a PsbQ' protein (the so-called 20 kDa protein) in non-green algal PSII preparations (*16*).

In this study, we have paid special attention to one of the three extrinsic proteins of higher plants, PsbQ. The spinach PsbQ protein consists of 149 amino acids (~17 kDa) with a basic p*I* of 9.2 (*17*). The consensus sequence of the PsbQ family has a single, fully conserved tryptophan residue, and contains many glycine and proline residues, especially in the N-terminal region (*18*). Recently, ~70% of the 3D structure of PsbQ from spinach has been obtained at 1.95 Å (*19*). In parallel, a structural threading model was also proposed (*20*) that agrees well with the X-ray model. The partial 3D structure of the PsbQ protein shows a single domain with a four α-helical up-down bundle folding at the C-terminus and a region of partially non canonical structure at the N-terminus, which is proposed to be involved in the binding to PSII (*21*). However, little is yet known about the specific function and structural stability of PsbQ.

A thermodynamic study on PsbQ is thus of interest, since changes in its native conformation could be translated into a loss of its biological function. In a first study, the FTIR thermal-denaturation study of the spinach PsbQ protein (*22*) showed that PsbQ is a stable protein (T_m~65 ºC). To our knowledge the work by Zhang and co-worker has been the only one reported on PsbQ thermostability so far. Since PsbQ is essential for a fully active PSII oxygen evolving complex and, moreover, oxygen evolution by PSII is known to be one of the most sensitive reactions to temperature rise in higher plants and algae (*23, 24*), we report here a more complete thermodynamic study on the structural stability and the unfolding/refolding process of the recombinant spinach PsbQ, by means of intrinsic protein fluorescence emission, far- and near-UV circular dichroism (CD), and differential scanning calorimetry (DSC). The quaternary structure of PsbQ and its hydrodynamic behavior are also investigated using analytical

ultracentrifugation. PsbQ structural stability will be discussed in terms of stability associated with PSII.

MATERIALS AND METHODS

Protein purification

The purification of recombinant spinach PsbQ protein was carried out as described by (*18*), and the purity checked by SDS-PAGE (*25*). The PsbQ protein concentration was determined in a Cary 100 UV-visible spectrophotometer. The molar absorption coefficient of PsbQ (14100 $M^{-1} \cdot cm^{-1}$) was calculated as the sum of the molar absorption coefficients of its aromatic amino acids at 276 nm in 6.0 M GdnHCl according to (*26*). PsbQ was stored at -80 ºC in 1 mM EDTA, 20 mM Tris-HCl pH 8.0 until use.

Buffers and solutions

All the reagents used in this study were of analytical grade. To cover a pH range between 2.0 and 8.0, sodium citrate-HCl (pH 2.0–3.5), sodium acetate-HCl (pH 4.0–5.0), KH_2PO_4/K_2HPO_4 (pH 6.0–7.0) and Tris-HCl (pH 8.0) were chosen as buffers and prepared at a final concentration of 50 mM. The GdnHCl stock solution was prepared as described by (*27*) and the final concentration was measured by refractometry.

Sedimentation equilibrium

Sedimentation equilibrium experiments were performed by centrifugation of 80 µl of 60 µM PsbQ in 1 mM EDTA, 20 mM Tris-HCl pH 8.0 at 110,000 g and 20 ºC in an Optima XL-A analytical ultracentrifuge (Beckman Coulter Instrument, Inc.), using 12 mm double-sector six-channel epon-charcoal centerpieces (AN50Ti rotor). Radial scans were taken at 280 nm at 12, 16 and 18 h with the same results. Baseline offsets were determined from absorbance near to the meniscus of a radial scan taken after running the sample for 8 h at 150,000 g. Conservation of

integral absorbance in the cell was checked in all the experiments. The apparent average molecular mass, M_{wapp}, was obtained by fitting a sedimentation equilibrium model for a single species to individual data sets, using the conservation of signal algorithm (*28*) from EQASSOC and XLAEQ programs. The partial specific volume of PsbQ calculated from its amino acid composition was 0.7398 $ml \cdot g^{-1}$.

Sedimentation velocity

The experiments were performed at 25 ºC and 150,000 g, using 400 µl of 60 µM PsbQ in 1 mM EDTA, 20 mM Tris-HCl pH 8.0. Radial scans at 280 nm were taken every 10 min. The sedimentation coefficients and their distributions were calculated with the SEDFIT program (*29*) and from the rate of the movement of: *i)* the solute boundary (XLAVEL program, Beckman) and *ii)* the second moment of the boundary (VELGAMMA program, Beckman). The experimental values were converted to standard conditions (*30*) to get the corresponding $s_{20,w}$ values. The hydrodynamic parameters were estimated by the v-bar method implemented in the SEDNTERP program to estimate the asymmetry of the PsbQ particles in solution (*31*). The axial ratio (*a*/*b*) for different particle models was calculated from the friction coefficient ratio, f/f_o, where f and f_o stand, respectively, for the experimental friction coefficient and the minimum friction coefficient assuming a spherical shape for the protein.

Circular dichroism

Thermal unfolding of PsbQ was monitored by far- and near-UV CD spectroscopy using a J-810 Jasco spectropolarimeter equipped with a Peltier temperature control unit, whereas GdnHCl-induced unfolding of PsbQ was characterized by far-UV CD at 20 ºC in a J-720 Jasco spectropolarimeter equipped with a refrigerated circulator (Neslab RTE-110). CD spectra were the average of two/four accumulations, using a scanning speed of 20 $nm \cdot min^{-1}$, 1 nm spectral bandwidth and a response time of 4 s. PsbQ protein concentrations were 10 µM or 90 µM, respectively, for the far- and near-UV region of the CD spectra. Quartz cuvettes of 1.0 and 10

mm path lengths were, respectively, chosen on the former and latter UV region. Thermal denaturation of PsbQ was characterized by measuring the ellipticity changes at 220 nm (far-UV) and 291 nm (near-UV) induced by temperature increase from 20 to 90 ºC at a heating rate of 20 ºC h^{-1}. Reversibility of PsbQ denaturation was assessed acquiring the CD spectra of the sample at the same initial condition after heating to 90 ºC at 20 ºC·h^{-1}. Far-UV CD denaturation plots for the PsbQ unfolding and refolding reactions in GdnHCl at 20 ºC were obtained by averaging the ellipticity value at 220 nm for 10 min for each GdnHCl concentration assayed. The buffer contribution was subtracted in all the experiments.

Fluorescence experiments

Fluorescence emission measurements were performed on a steady-state Photon Technology International spectrofluorometer, model QM-2000-4, equipped with a refrigerated circulator (Neslab RTE-210). Both excitation and emission monochromators were set at 3 nm slit widths. The tryptophan of PsbQ was excited at 295 nm. Fluorescence emission spectra (averaged 3 times) were recorded in a 0.5 cm path quartz cuvette from 300 to 500 nm with steps of 0.5 nm and an integration time of 2 s, and corrected by subtracting the Raman band and the buffer signal. The PsbQ concentration was kept at 5 μM. Chemically and thermally induced unfolding curves were obtained by measuring the fluorescence emission intensity at 320 nm between 0 and 6.0 M GdnHCl at 20 ºC, and between 20 and 90 ºC, respectively.

Differential scanning calorimetry (DSC)

Calorimetric measurements of PsbQ were performed in a Microcal MCS instrument. Typically, samples were scanned from 20 to 95 ºC at a heating rate of 20 ºC·h^{-1} under a constant pressure of 2 atm. The standard MCS and Microcal Origin software were used for data acquisition and analysis. After baseline subtraction of the buffer-buffer signal, the molar excess heat capacity function was obtained dividing by the protein concentration and the cell volume (1.204 mL). Reversibility of the PsbQ protein denaturation was assessed by comparing two consecutive

scans of the same sample. Aliquots of stock solutions of PsbQ at 60–180 μM were extensively dialyzed against the buffer employed at each pH before any DSC experiment.

Data analysis

Chemical unfolding. For a two-state unfolding process (N↔D), the free energy of chemical unfolding in the transition region has been found to be linearly dependent on the denaturant concentration according to (*27*). The free energy of unfolding, ΔG_D, and the value of the spectroscopic property measured, y, are related by the equation:

$$y = y_D - (y_D - y_N) / \left\{1 + \exp\left(\Delta G_D^{H_2O} - m \cdot [GdnHCl] / RT\right)\right\} \qquad [1]$$

where y_N and y_D are, respectively, the ellipticity values or the fluorescence intensity of the native and denatured states of the protein, m is the slope of ΔG_D as a function of the denaturant concentration, $\Delta G_D^{H_2O}$ is the structural stability of the protein at zero denaturant concentration obtained by linear extrapolation and R is the gas constant. Both y_N and y_D were linearly dependent on GdnHCl concentration. The subsequent substitution of y_N and y_D in equation [1] led to the determination of the thermodynamic parameters m and $\Delta G_D^{H_2O}$ by a non-linear square regression fitting of the experimental data.

Spectroscopic thermal unfolding curves. For a two-state reversible unfolding, the dependence of the spectroscopic property measured with temperature is given by the equation:

$$y = y_D - (y_D - y_N) / \left[1 + \exp\left(\Delta H_D^{vH} (T - T_m) / RT_m T\right)\right] \qquad [2]$$

where y, y_N and y_D are defined as above, T_m is the melting temperature, $\Delta G_D(T_m)=0$, and ΔH_D^{vH} is the enthalpy change for the unfolding transition at T_m. Substitution of y_N and y_D in

equation [2] by their temperature dependent function led to the determination of the thermodynamic parameters T_m and ΔH_{vH} by a non-linear square regression fitting of the experimental data.

Calorimetry. The denaturation temperature, T_m, and the calorimetric denaturation enthalpy change, ΔH_D, were determined by analyzing the excess heat capacity functions with MicroCal DSC Origin software in terms of both non-two state and two-state transitions. The ratio between the calorimetric and the van´t Hoff enthalpy changes, $\Delta H_D / \Delta H_D^{vH}$, is a measure of the extent to which a protein unfolding deviates from the two-state model (*32*). Thus, a value of $\Delta H_D / \Delta H_D^{vH}$ close to unity indicates the validity of the assumption of a two-state transition. For a reversible protein unfolding according to the two-state model -which is stable in the denatured state and has a constant denaturation heat capacity change- the temperature dependence of protein stability can be obtained from the Gibbs-Helmholtz equation (*33*).

RESULTS

PsbQ is a monomer in solution

The theoretical molecular mass of the recombinant spinach PsbQ protein calculated from the amino acid sequence is 16.65 kDa. The sedimentation velocity experiments of PsbQ in 20 mM Tris-HCl pH 8.0 indicated the presence of a single component (**Figure 1A**) with a standard sedimentation coefficient, $s_{20,w}$, of 1.42 ± 0.05 S and a diffusion coefficient, D, of (7.8±0.1)×10^{-7} $cm^2 \cdot s^{-1}$, which point to an elongated shape for PsbQ in solution according to (*34*). Using these parameters and the partial specific volume of PsbQ ($\bar{\upsilon}$ = 0.7398 $mL \cdot g^{-1}$), the calculated value of the molecular mass of PsbQ by the Svedberg equation (*30*) was 16.7 kDa, very close to the molecular mass of the monomeric PsbQ protein (16.65 kDa). The same results were found in potassium phosphate buffer (data not shown). The equilibrium sedimentation experiments confirmed that neither aggregation nor oligomerization of PsbQ occurs in solution under our

experimental conditions (**Figure 1B**), although a very slight deviation from ideality was found when fitting the plot to a single protein species. Thus, the PsbQ protein was proposed to exist as a monomer in solution. The friction coefficient ratio, f/f_o, was calculated to be 1.6, suggesting also that PsbQ behaves as an elongated protein in solution. Assuming a protein hydration degree of 0.4307 g of H_2O per g of protein according to (*35*), the f/f_0 value is compatible with either a prolate ellipsoid of revolution with an axial ratio of 6.7 and axis lengths of 14 and 2.1 nm; or an oblate ellipsoid of revolution with an axial ratio of 7.7 and axis lengths of 7.8 and 1.0 nm.

Chemically induced denaturation of PsbQ

Figure 2A shows the far-UV CD spectra of PsbQ in the concentration range of 0–6.0 M GdnHCl (pH 8.0) at 20 ºC. The far-UV CD spectrum of native PsbQ exhibits a strong positive band peaking at 193 nm and two negative ones at 209 and 219 nm (*18*). On increasing the GdnHCl concentration in the PsbQ solution, a concomitant decrease in the ellipticity at 220 nm was observed, suggesting a cooperative loss of the α-helix content in PsbQ. At 6.0 M GdnHCl, the far-UV CD spectrum of PsbQ is characteristic of a protein that has lost its secondary structure. On the other hand, the refolding of PsbQ revealed that chemical denaturation by GdnHCl was a reversible process (**Figure 2 A,B**). The 220 nm-normalized unfolding/refolding far-UV CD plots of PsbQ showed a single transition between 0.2 M and 1.2 M, with a $[GdnHCl]_{1/2}$ of 0.8 M **(Figure 2B)**. The calculation of the free energy of both unfolding and refolding, assuming a two-state mechanism, yielded average values of $\Delta G_D^{H_2O} = 4\pm1$ kcal·mol^{-1} and $m = 5\pm1$ kcal·mol^{-1}·M^{-1} at 20 ^{0}C, when fitting equation [1] to the two experimental data sets. Chemical unfolding of PsbQ was also monitored by measuring specifically the intrinsic fluorescence emission of its single fully conserved tryptophan residue. On exciting at 295 nm, incubation of PsbQ with increasing concentrations of GdnHCl (up to 6.0 M) resulted in a significant bathochromic shift of its fluorescence emission maximum, from 327 nm to 353 nm, and also in a severe quenching of its fluorescence emission intensity (**Figure 2C**). This bathochromic shift is consistent with the exposure of tryptophan to the solvent upon

denaturation. The finding of an isostilbic point at 372 nm in the set of fluorescence emission spectra suggests that the GndHCl denaturation of PsbQ behaves as a two-state process. On monitoring the fluorescence emission at 320 nm at increasing concentrations of GdnHCl, a single and sharp transition was observed with a $[GdnHCl]_{1/2}$ of 0.8 M **(Figure 2D)**. The values of $\Delta G_D^{H_2O}$ = 3.9±0.2 kcal·mol^{-1} and *m*= 5.0±0.2 kcal·mol^{-1}·M^{-1} obtained by fitting the experimental curves in terms of equation [1] were in excellent agreement with those derived from the far-UV CD analysis.

Thermally induced denaturation of PsbQ.

The heating effect on the secondary structure of PsbQ was studied by far-UV CD (**Figure 2E).** On increasing the temperature from 20 to 90 ºC, the evolution of the far-UV CD spectra of PsbQ revealed a decrease in the overall ellipticity and the presence of isodichroic point at 204 nm, pointing both to a cooperative loss of the α-helix structure of PsbQ and to a two-state transition. The far-UV CD spectrum of PsbQ at 90 ºC was also found to be very similar to that obtained in 6.0 M GdnHCl at 90 ºC (data not shown), suggesting that both chemically and thermally denatured states of PsbQ possess an equivalent residual secondary structure. To correlate changes in secondary structure with those in tertiary structure, thermally induced denaturation was also studied by intrinsic fluorescence emission and near-UV CD. On exciting specifically the tryptophan at 295 nm, the intrinsic fluorescence emission spectra of PsbQ exhibited a significant bathochromic shift of its maximum, from 327 to 352 nm, and also a severe quenching of its fluorescence emission intensity when rising the temperature from 20 to 90 ºC (data not shown). These changes in the intrinsic fluorescence emission spectrum of PsbQ are very similar to those previously described for the GdnHCl-induced denaturation, suggesting that in both cases the tryptophan is equally exposed to the solvent in the final unfolded state of PsbQ. The near-UV CD spectra also revealed a loss of PsbQ tertiary structure upon heating from 20 to 90 ºC, showing a cooperative change of its fine features into blunt ones (**Figure 2G**). More than 90% of the initial ellipticity in both far- and near-UV CD spectra, and the initial

intensity in the fluorescence emission spectra were restored when cooling back the PsbQ solutions to 20 ºC. On monitoring the ellipticity at 220 nm (far UV CD) and at 291 nm (near UV CD), and the fluorescence intensity at 320 nm (data not shown), the thermal denaturation of PsbQ exhibits a cooperative sigmoidal behavior, which begins at 55 ºC and is nearly complete at 75 ºC (**Figure 2F, 2H).** Similar results were obtained using potassium phosphate buffer pH 8.0 (data not shown). The thermal denaturation parameters were further calculated by a non-linear fitting of the transition plots using equation [2]. These values were as follows: T_m = 63.0 ± 0.1 ºC and ΔH_D^{vH} = 69 ± 2 kcal·mol^{-1} (far-UV CD); T_m = 63.5 ± 0.5 ºC and ΔH_D^{vH} = 69 ± 4 kcal·mol^{-1} (near-UV CD); and T_m = 62.9 ± 0.2 ºC and ΔH_D^{vH} = 74 ± 3 kcal·mol^{-1} (fluorescence emission).

Calorimetric measurements

Figure 3A shows the temperature dependence of the excess heat capacity of PsbQ in 20 mM Tris-HCl pH 8.0. The thermogram shows a single and sharp endothermic peak at 64.8 ± 0.1 ºC and a value for ΔH_D= 61.3 ± 0.8 kcal·mol^{-1}. On scanning the PsbQ solution a second time, the thermogram showed that the refolding of PsbQ was 70–85 % reversible (**Figure 3B**) or even completely reversible if the first scan was intentionally stopped around the T_m (**Figure 3B, 3C**). In addition, the thermogram does not depend on the scan rate (data not shown), suggesting that irreversible denaturation of PsbQ only takes place significantly at temperatures above the transition region. The analysis of the heat capacity curve yields values of about 0.85 for the $\Delta H_D / \Delta H_D^{vH}$ ratio, indicating that the process was slightly more cooperative than expected for a two-state transition. Since PsbQ is a monomer and the thermograms were independent of protein concentration (data not shown) the value of $\Delta H_D / \Delta H_D^{vH}$ could reflect some protein aggregation at temperatures well above the T_m. **Figure 4** summarizes the evolution of the thermal denaturation of PsbQ as monitored by DSC, CD and fluorescence. The very close overlap among all the denaturated fractions of PsbQ, each determined by a different technique,

in 20 mM Tris-HCl pH 8.0, strongly supports the notion that denaturation of PsbQ can be described in terms of a two-state transition.

Influence of pH on protein stability

Denaturation of PsbQ with temperature has also been characterized by near- and far-UV CD and DSC at various pH. A first analysis showed that far- and near-UV CD spectra of PsbQ were coincident, within experimental error, between pH 2.0 and 8.0, discarding any affect of pH on the secondary and tertiary structure of PsbQ at 20º C (data not shown). In addition, no dependence on ionic strength was found. However, the thermal stability of PsbQ was seen to be pH dependent. The transition temperature remains almost constant between pH 8.0 and 5.0, but severely decreases on decreasing pH beyond 5.0 **(Figure 5A,C; Table 1).** Similar results were obtained by DSC (**Figure 5B,C).** The heat capacity change accompanying denaturation of PsbQ was estimated from the temperature dependence of ΔH_D values (ΔH_{vH}^D for CD measurements) obtained at different pH. The slope of the linear plot resulted in ΔCp_D = 1.2 ± 0.4 kcal·mol^{-1}·K^{-1} (**Figure 5D**). By means of the Gibbs-Helmholtz equation, the structural stability of PsbQ in 20 mM Tris-HCl pH 8.0 was estimated to be 4.4 ± 0.8 kcal·mol^{-1} at 20 ºC.

DISCUSSION

In this work we have advanced in the knowledge of the small extrinsic PsbQ protein of PSII. The hydrodynamic and thermodynamic characterization of PsbQ was performed with the aim of knowing its N-mer state (quaternary structure), as well as the structural stability in solution, and its dependence on pH. By means of CD and fluorescence spectroscopies and DSC, both secondary and tertiary structures have been used as probes to analyze PsbQ denaturation and calculate the unfolding thermodynamic parameters.

The experimental molecular mass determined by analytical ultracentrifugation was in excellent agreement with the monomer molecular mass drawn from the PsbQ sequence. Both sedimentation velocity and equilibrium experiments show that isolated PsbQ behaves as a

homogeneous monomeric particle in solution at 20 ºC, since no evidence for dimers or larger oligomers was found in the sedimentation coefficient distribution function of PsbQ. This fact might be of physiological relevance. The extrinsic proteins of higher plant PSII—PsbO, PsbP and PsbQ—are proposed to be bound in a 1:1:1 stoichiometry to the luminal side of PSII (*8*). However, they can dissociate from PSII under stress conditions such as low pH or high temperature (*36, 37*), remaining temporarily in the thylakoid lumen where they are stable (*38*). Upon returning the optimal physiological conditions for oxygen evolution, they all rebind to PSII. The fact that the free PsbQ remains as a monomer in solution could facilitate both the specific protein-protein interactions with the other extrinsic proteins, and also the right docking at the luminal side of PSII**.** On the contrary, oligomerization of PsbQ in the thylakoid lumen could result in a loss of functionality or even in a signal for proteolytic degradation.

The structural stability of PsbQ was analyzed by denaturation with GdnHCl, high temperature, or combining both high temperature and low pH. The superposition of the normalized fluorescence- and CD-monitored unfolding curves of PsbQ at increasing GdnHCl concentrations, each of which can be fitted to a reversible two-state equation, indicates that PsbQ behaves as a single cooperative unit upon chemical denaturation. The unfolding curves measured by the two probes have, within error, the same value of 0.8 M for the $[GdnHC]_{1/2}$. The isostilbic point in the series of tryptophane fluorescence emission spectra further supports the two-state model. The average thermodynamic parameters obtained (m = 5.0±0.6 kcal·mol^{-1}·M^{-1} and $\Delta G_D^{H_2O}$ = 4.0±0.6 kcal·mol^{-1}) are in the range of those reported for globular proteins of similar molecular mass (*39*), though a small deviation is seen in PsbQ based on its elongated shape.

Thermal denaturation of PsbQ was found to be more than 90% reversible as testing by refolding of the denatured protein monitored by CD and by tryptophan fluorescence spectroscopies. The reversibility of DSC transitions was somewhat lower (around 70–85%) upon heating above the transition temperature range. However, the fact that PsbQ denaturation was almost fully reversible up to temperatures around the T_m is consistent with the

independence of thermal DSC scans on the heating rate, and suggests that irreversibility appears at the end and beyond the transition region. On the other hand, the differences in reversibility found between DSC and the two spectroscopic probes suggest that there might be some PsbQ regions that scarcely contribute to the CD and the fluorescence spectra of the protein. It is worth noting that PsbQ has a non canonical secondary structure in the N-terminal region comprising residues 1–45 (*20*), difficult to evaluate by far- and near-UV CD, and with a very high content in proline residues, whose isomerization might impair the protein refolding. As with chemically induced unfolding, thermal denaturation of PsbQ can also be described as a two state process according to the spectroscopic-probe transition curves. The model is also supported by the isodichroic point in the series of far UV CD spectra registered at increasing temperatures, and the overlapping, within experimental error, of the denatured fraction plots of PsbQ, determined by far- and near-UV CD, intrinsic fluorescence and DSC. They all show one single transition with a coincident T_m around 63 ºC (**Figure 4**). The slight deviation of calorimetric profiles from the two-sate model at basic pH ($\Delta H_D / \Delta H_D^{vH}$= 0.85 at pH 8.0) could be due to some protein aggregation at temperatures beyond the T_m since DSC transition was practically independent of PsbQ concentration. Such an effect would be expected to be more pronounced as the pH approaches the p*I* of PsbQ (9.25), which is in agreement with the experimental results ($\Delta H_D / \Delta H_D^{vH}$ = 0.97 at pH 2–4). Whatever the case, the thermodynamic analysis of PsbQ in the transition region is not significantly affected by these processes occurring well above the transition temperature. The dependence of T_m on pH allowed us to estimate the denaturation heat capacity change (ΔCp_D = 1.2± 0.4 cal·mol^{-1}·K^{-1}), necessary to calculate the temperature dependence of PsbQ stability. The extrapolation of the free energy change between the denatured and the native states, ΔG_D, at 20^{0}C and pH 8.0 yielded a value of 4.4±0.8 kcal·mol^{-1}, in good agreement with the $\Delta G_D^{H_2O}$ derived from GdnHCl denaturation at the same pH and fall into the range observed for other proteins (*40*).

Our study shows that there are no structural changes in PsbQ within the pH range 2.0–8.0. However, the stability of isolated PsbQ severely decreases at pH values below 5.0,

remaining rather stable at pH values comprised between 5–8. Interestingly, the pH of maximum stability of PsbQ is wider than the narrow optimal pH for oxygen evolution in the lumen (5.5–6.5). In a previous study (*36*), PsbQ was proposed to be 50% released from PSII after 30 min of incubation at pH 5.0. This dissociation process seems to be unassociated with PsbQ unfolding, since no significant structural changes in its secondary or tertiary structure have been detected upon lowering pH. However, considering the non canonical secondary structure of PsbQ N-terminal region we cannot fully rule out that subtle structural changes in this N-terminus might be responsible for its dissociation from PSII at acidic pH, given the essential role of this region for PsbQ binding to PSII (*41*). Alternatively, changes in the protonation state of PsbQ, not affecting its conformational state, could also explain the PsbQ detachment from PSII at acidic pH. In this case, the pK_a of the PsbQ residue(s) directly implicated in the protein binding to PSII should be near 5.0, to explain the approximately 50% dissociation of PsbQ at pH 5.0 reported by Shen and Inoue (1991). This pK_a value could be assigned to carboxylic groups whose negative charges are stabilized by micro environmental conditions or by implication in strong buried salt-bridges with residues belonging either to PsbQ or to another subunit of PSII (*42*). It is worth noting the strong polarity observed in the charge distribution within the PsbQ family of proteins, with isoelectric points of 4.47 and 9.49, respectively, for the N-terminal (residues 1–45) and C-terminal (residues 46–149) regions in spinach (*20*). According to this, the net charge of the N-terminus would be strongly modified in the pH interval where PsbQ dissociates from PSII, and suggests that negatively charged residues of the N-terminal region could play a key role in PSII-PsbQ interactions given the implication of this region in PsbQ binding to PSII. The relevance of electrostatic forces for PsbQ-PSII interactions is supported by the PsbQ dissociation from PSII at high salt concentration (*8*)**.** Nevertheless, structural changes in other intrinsic or extrinsic subunits of PSII at acidic pH could also be involved in PsbQ dissociation from PSII.

Upon incubation of the thylakoids or the PSII-enriched membranes of green algae or higher plants at 40–50 ºC for only 5 min, the three extrinsic proteins—PsbO, PsbP and PsbQ—

are released from PSII resulting in a fully inactive oxygen-evolving complex (*45, 46*). Likewise, it is well known that under high light stress, there is an over-acidification of the thylakoid lumen leading to energy de-excitation by non-photochemical quenching that photoprotect green algal and higher plant PSII (*47, 48*). The low pH of the thylakoid lumen also induces the release of the three extrinsic proteins from PSII (36). According to our current *in vitro* results, PsbQ detachment by heat or pH is not expected to be associated with protein denaturation, since no significant loss of ellipticity is seen in the far- and near-UV CD spectra at temperatures below 50 ºC or pH´s between 2 and 8. In this way, PsbQ could be in a soluble and stable state in the thylakoid lumen, probably prepared for an efficient re-binding to PSII. Upon recovery of the optimal physiological conditions (temperature and/or pH) for oxygen evolution, the extrinsic proteins rebind to the luminal side of PSII, resuming water oxidation. The natural choice of weakly binding extrinsic proteins—PsbO, PsbP and PsbQ—to algal and higher plant PSII is not yet well understood, but it could be part of a molecular mechanism against photoinhibition in higher plants.

In conclusion, PsbQ is a homogeneous, monomeric protein with an elongated shape in solution. The denaturation process induced by GdnHCl or temperature involves a cooperative, reversible classical two-state mechanism where only the native and the denatured state are significantly populated. Its maximum stability is in the pH range between 5 and 8 that is wider than the one for optimal water oxidation at the luminal side of PSII.

REFERENCES

1. Barber, J. (2003) Photosystem II: the engine of life, *Q. Rev. Biophys. 36*, 71–89.
2. Diner, B. A., and Rappaport, F. (2002) Structure, dynamics, and energetics of the primary photochemistry of photosystem II of oxygenic photosynthesis, *Annu. Rev. Plant Biol. 53*, 551–580.
3. Goussias, C., Boussac, A., and Rutherford, A. W. (2002) Photosystem II and photosynthetic oxidation of water: an overview, *Philos. Trans. R. Soc. Lond. B. Biol. Sci. 357*, 1369–1381.

4. Zouni, A., Witt, H. T., Kern, J., Fromme, P., Krauss, N., Saenger, W., and Orth, P. (2001) Crystal structure of photosystem II from *Synechococcus elongatus* at 3.8 Å resolution, *Nature 409*, 739–743.

5. Kamiya, N., and Shen, J. R. (2003) Crystal structure of oxygen-evolving photosystem II from *Thermosynechococcus vulcanus* at 3.7 Å resolution, *Proc. Natl. Acad. Sci. U. S. A. 100*, 98–103.

6. Ferreira, K. N., Iverson, T. M., Maghlaoui, K., Barber, J., and Iwata, S. (2004) Architecture of the photosynthetic oxygen-evolving center, *Science 303*, 1831–1838.

7. Rutherford, A. W., and Faller, P. (2003) Photosystem II: evolutionary perspectives, *Philos. Trans. R. Soc. Lond. B Biol. Sci. 358*, 245–253.

8. Seidler, A. (1996) The extrinsic polypeptides of photosystem II, *Biochim. Biophys. Acta 1277*, 35–60.

9. De Las Rivas, J., Balsera, M., and Barber, J. (2004) Evolution of oxygenic photosynthesis: genome-wide analysis of the OEC extrinsic proteins, *Trends Plant Sci. 9*, 18–25.

10. Miyao, M., and Murata, N. (1984) Role of the 33-kDa protein in preserving Mn in the photosynthetic oxygen-evolution system and its replacement by chloride ions, *FEBS Lett. 170*, 350–354.

11. Vrettos, J. S., Limburg, J., and Brudvig, G. W. (2001) Mechanism of photosynthetic water oxidation: combining biophysical studies of photosystem II with inorganic model chemistry, *Biochim. Biophys. Acta 1503*, 229–245.

12. Wincencjusz, H., Yocum, C. F., and van Gorkom, H. J. (1999) Activating anions that replace Cl^- in the O_2-evolving complex of photosystem II slow the kinetics of the terminal step in water oxidation and destabilize the S_2 and S_3 states, *Biochemistry 38*, 3719–3725.

13. Vander Meulen, K. A., Hobson, A., and Yocum, C. F. (2002) Calcium depletion modifies the structure of the photosystem II O_2-evolving complex, *Biochemistry 41*, 958–966.

14. Thornton, L. E., Ohkawa, H., Roose, J. L., Kashino, Y., Keren, N., and Pakrasi, H. B. (2004) Homologs of Plant PsbP and PsbQ Proteins Are Necessary for Regulation of Photosystem II Activity in the Cyanobacterium Synechocystis 6803, *Plant Cell 16*, 2164–75

15. Kashino, Y., Lauber, W. M., Carroll, J. A., Wang, Q., Whitmarsh, J., Satoh, K., and Pakrasi, H. B. (2002) Proteomic analysis of a highly active photosystem II preparation from the cyanobacterium *Synechocystis* sp. PCC 6803 reveals the presence of novel polypeptides, *Biochemistry 41*, 8004–8012.

16. Ohta, H., Suzuki, T., Ueno, M., Okumura, A., Yoshihara, S., Shen, J. R., and Enami, I. (2003) Extrinsic proteins of photosystem II: an intermediate member of PsbQ protein family in red algal PS II, *Eur. J. Biochem. 270*, 4156–4163.

17. Jansen, T., Steppuhn, R. C. J., Reinke, H., Beyreuther, K., and Jansson, C. (1987) Nucleotide sequence of cDNA clones encoding the complete '23 kDa' and '16 kDa' precursor proteins associated with the photosynthetic oxygen-evolving complex from spinach., *FEBS Lett. 216*, 234–240.

18. Balsera, M., Arellano, J. B., Gutierrez, J. R., Heredia, P., Revuelta, J. L., and De Las Rivas, J. (2003) Structural analysis of the PsbQ protein of photosystem II by Fourier transform infrared and circular dichroic spectroscopy and by bioinformatic methods, *Biochemistry 42*, 1000–1007.

19. Calderone, V., Trabucco, M., Vujicic, A., Battistutta, R., Giacometti, G. M., Andreucci, F., Barbato, R., and Zanotti, G. (2003) Crystal structure of the PsbQ protein of photosystem II from higher plants, *EMBO Rep. 4*, 900–905.

20. Balsera, M., Arellano, J. B., Pazos, F., Devos, D., Valencia, A., and De Las Rivas, J. (2003) The single tryptophan of the PsbQ protein of photosystem II is at the end of a 4-alpha-helical bundle domain, *Eur. J. Biochem. 270*, 3916–3927.

21. Kuwabara, T., and Suzuki, K. (1994) A prolyl endoproteinase that acts specifically on the extrinsic 18-kDa protein of photosystem-II: purification and further characterization, *Plant Cell Physiol. 35*, 665–675.

22. Zhang, H., Yamamoto, Y., Ishikawa, Y., and Carpentier, R. (1999) Characterization of the secondary structure and thermostability of the extrinsic 16 kilodalton protein of spinach photosystem II by Fourier transform infrared spectroscopy, *J. Mol. Struct. 513*, 127–132.

23. Nash, D., Miyao, M., and Murata, N. (1985) Heat inactivation of oxygen evolution in photosystem-II particles and its acceleration by chloride depletion and exogenous manganese, *Biochim. Biophys. Acta 807*, 127–133.

24. Yamashita, T., and Butler, W. L. (1968) Inhibition of chloroplasts by UV-irradiation and heat-treatment, *Plant Physiol. 43*, 2037–2040.

25. Laemmli, U. K. (1970) Cleavage of structural proteins during the assembly of the head of bacteriophage T4, *Nature 227*, 680–685.

26. Gill, S. C., and von Hippel, P. H. (1989) Calculation of protein extinction coefficients from amino acid sequence data, *Anal. Biochem. 182*, 319–326.

27. Pace, C. N. (1986) Determination and analysis of urea and guanidine hydrochloride denaturation curves, *Methods Enzymol. 131*, 266–280.

28. Minton, A. P. (1994) in *Modern analytical ultracentrifugation* (Schuster, T. H., and Lave, L., Eds.) pp 81–92, Birkhaüser, Boston.

29. Schuck, P. (2000) Size-distribution analysis of macromolecules by sedimentation velocity ultracentrifugation and Lamm equation modeling, *Biophys. J. 78*, 1606–1619.

30. Lebowitz, J., Lewis, M. S., and Schuck, P. (2002) Modern analytical ultracentrifugation in protein science: a tutorial review, *Protein Sci. 11*, 2067–2079.

31. Laue, T. M., Shah, B.D., Ridgeway, T.M., and Pelletier, S.L. (1992) in *Analytical ultracentrifugation in biochemistry & polymer science* (Harding, S. E., Horton, H. C., and Rowe, A. J., Eds.) pp 90–125, Royal Society of Chemistry, London.

32. Privalov, P. L. (1979) Stability of proteins: small globular proteins, *Adv. Protein Chem. 33*, 167–241.

33. Becktel, W. J., and Schellman, J. A. (1987) Protein stability curves, *Biopolymers 26*, 1859–1877.

34. Selivanova, O. M., Shiryaev, V. M., Tiktopulo, E. I., Potekhin, S. A., and Spirin, A. S. (2003) Compact globular structure of *Thermus thermophilus* ribosomal protein S1 in solution - Sedimentation and calorimetric study, *J. Biol. Chem. 278*, 36311–36314.

35. Pessen, H., and Kumosinski, T. F. (1985) Measurements of protein hydration by various techniques, *Methods Enzymol. 117*, 219–255.

36. Shen, J. R., and Inoue, Y. (1991) Low pH-induced dissociation of 3 extrinsic proteins from O_2-evolving photosystem-II, *Plant Cell Physiol. 32*, 453–457.

37. Yamane, Y., Kashino, Y., Koike, H., and Satoh, K. (1998) Effects of high temperatures on the photosynthetic systems in spinach: Oxygen-evolving activities, fluorescence characteristics and the denaturation process, *Photosynth. Res. 57*, 51–59.

38. Kieselbach, T., and Schröder, W. P. (2003) The proteome of the chloroplast lumen of higher plants, *Photosynth. Res. 78*, 249–264.

39. Myers, J. K., Pace, C. N., and Scholtz, J. M. (1995) Denaturant *m* values and heat capacity changes: relation to changes in accesible surface areas of protein unfolding, *Protein Sci. 4*, 2138–2148.

40. Pace, C. N. (1990) Measuring and increasing protein stability, *Trends Biotechnol. 8*, 93–98.

41. Kuwabara, T., Murata, T., Miyao, M., and Murata, N. (1986) Partial degradation of the 18-kDa protein of the photosynthetic oxygen-evolving complex - a study of a binding-site, *Biochim Biophys Acta 850*, 146–155.

42. Yang, A. S., and Honig, B. (1993) On the pH dependence of protein stability, *J. Mol. Biol. 231*, 459–474.

43. Nishiyama, Y., Los, D. A., Hayashi, H., and Murata, N. (1997) Thermal protection of the oxygen-evolving machinery by PsbU, an extrinsic protein of photosystem II, in *Synechococcus* species PCC 7002, *Plant Physiol. 115*, 1473–1480.

44. Kimura, A., Eaton-Rye, J. J., Morita, E. H., Nishiyama, Y., and Hayashi, H. (2002) Protection of the oxygen-evolving machinery by the extrinsic proteins of photosystem II is essential for development of cellular thermotolerance in *Synechocystis* sp. PCC 6803, *Plant Cell Physiol. 43*, 932–938.

45. Enami, I., Kitamura, M., Tomo, T., Isokawa, Y., Ohta, H., and Katoh, S. (1994) Is the primary cause of thermal inactivation of oxygen evolution in spinach PSII membranes release of the extrinsic 33 kDa protein or of Mn?, *Biochim Biophys Acta 1186*, 52–58.

46. Pueyo, J. J., Alfonso, M., Andres, C., and Picorel, R. (2002) Increased tolerance to thermal inactivation of oxygen evolution in spinach Photosystem II membranes by substitution of the extrinsic 33-kDa protein by its homologue from a thermophilic cyanobacterium, *Biochim. Biophys. Acta 1554*, 29–35.

47. Demming-Adams, B., and Adams, W. W. I. (1996) Photoprotection and other responses of plants to high light stress, *Annu. Rev. Plant. Physiol. Plant Mol. Biol. 43*, 599–626.

48. Niyogi, K. K. (1999) Photoprotection revisited: genetic and molecular approaches, *Annu. Rev. Plant. Physiol. Plant. Mol. Biol. 50*, 333–359.

49. Eskling, M., Arvidsson, P. O., and Åkerlund, H. E. (1997) The xanthophyll cycle, its regulation and components, *Physiol. Plant. 100*, 806–816.

Table 1. PsbQ thermodynamic parameters obtained by DSC at different pH values.

pH	T_m (ºC)	ΔH_D (kcal·mol^{-1})	ΔH_D^{vH} (kcal·mol^{-1})	$\Delta H_D / \Delta H_D^{vH}$
2.0	52.5 ± 0.1	54.2 ± 0.5	55.8 ± 0.7	0.97
4.0	62.6 ± 0.04	70.0 ± 0.5	73.2 ± 0.7	0.96
6.0	64.5 ± 0.03	64.6 ± 0.4	70.1 ± 0.6	0.92
8.0	64.8 ± 0.8	61.3 ± 0.8	71.6 ± 1.1	0.85

FIGURE LEGENDS

Figure 1. Sedimentation velocity and equilibrium experiments. (A) Sedimentation coefficient distribution of PsbQ in 20 mM Tris-HCl pH 8.0 at 20 ºC. (B) Upper panel: Variation of absorbance values of PsbQ at 280 nm on radial distance at 110,000 g; buffer and temperature as in A. The solid line is the plot fitting to a single protein model. Lower panel: distribution of residuals.

Figure 2. GdnHCl- and thermally-induced denaturation of PsbQ. (**A**) and (**C**) represent GdnHCl-induced variations in the far-UV CD and fluorescence emission spectra of PsbQ, respectively. Excitation wavelength, 295 nm. GdnHCl concentrations were from top to bottom as follows: 6.0, 0.9, 0.6 and 0 M (panel A) and 0, 0.3, 0.5, 0.7, 0.8, 1.0 and 2.0 M (panel C). Reversibility of GndHCl-induced denaturation was assessed by diluting 50 times the 6.0 M GdnHCl solution of PsbQ (open circles in panel A); (**B**) and (**D**) represent GndHCl-denaturation (filled square) and renaturation (open circle) plots at 220 nm and 320 nm obtained by far-UV CD and fluorescence emission, respectively, at 20 ºC. The regression fitting by equation [2] is indicated by a continuous line. (**E**) and (**G**) represent the temperature dependence (20–90 ºC) of far- and near-UV CD spectra of PsbQ, respectively. Temperatures were from top to bottom as follows: 90, 75, 70, 65, 60, 32 and 20 ºC (panel E) and 20, 40, 59, 63, 67 and 85 ºC (panel G). Reversibility was assessed by acquiring the CD spectra of the PsbQ protein under renaturing conditions after heating to 90 ºC at 20 ºC h^{-1}(open circle in both panels); (**F**) and (**H**) represent denaturation (filled square in both panels) plots at 220 nm and 292 nm obtained by far- and near-UV CD, respectively, from 20 to 90 ºC. The regression fitting by equation [2] is indicated by the continuous lines. GdnHCl concentrations or temperatures at which the CD or fluorescence emission spectra on the left hand side panels are recorded can be inferred from their counterpart ones on the right hand side.

Figure 3. DSC thermograms of PsbQ in 20 mM Tris-HCl pH 8.0. (**A**) Experimental molar excess heat capacity function (solid line) and the corresponding fitting to a non-two state transition model by Microcal software (dotted line) using data reported in Table I. The transition shows a single, sharp endothermic peak. (**B**) Reversibility experiments: Two consecutive scans of the same sample of PsbQ results in a reversibility of 70–85%. The superposition of the first scan (solid line) and the second scan (dotted line) points to irreversibility processes at high temperatures. (**C**) The reversibility is nearly 100% when heating is stopped around T_m in the first scan (solid line) and the second scan is run afterwards (dotted line).

Figure 4. Superposition of the apparent fraction of thermally denatured PsbQ estimated from the fluorescence emission (open square), far- and near-UV CD (filled triangle and open triangle, respectively) and DSC (open circle) denaturation experiments.

Figure 5. pH dependence of PsbQ thermal stability. (A) Far-UV CD denaturation plots at 220 nm (pH 2.0, 3.0, 4.0 and 6.0, from left to right); (B) DSC thermograms at pH 2.0, 4.0 and 6.0, from left to right. (C) Dependence of T_m on pH measured by DSC (filled circle) and far-UV CD (filled square). (D) Temperature dependence of ΔH_D (filled circle) and ΔH_D^{vH} (open circle) values obtained by DSC, and of ΔH_D^{vH} (filled square) values obtained by far-UV CD in the pH range of 2.0–8.0.

For Table of Contents Use Only

Structural stability of the PsbQ protein of higher plant photosystem II

Mónica Balsera, Margarita Menéndez, José L. Sáiz, Javier de las Rivas, José M. Andreu, and Juan B. Arellano

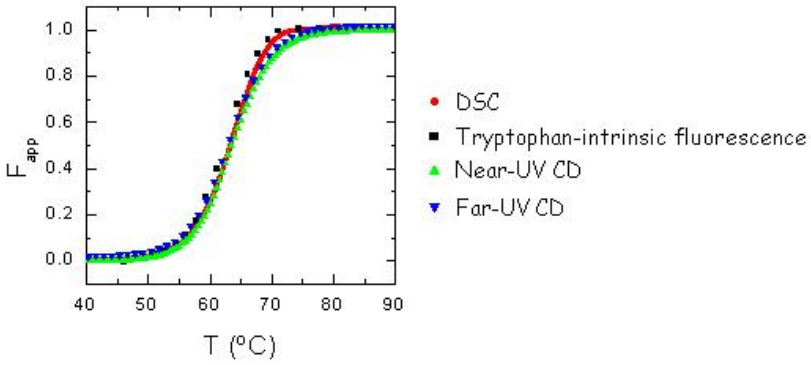

Balsera *et al.* Figure 1

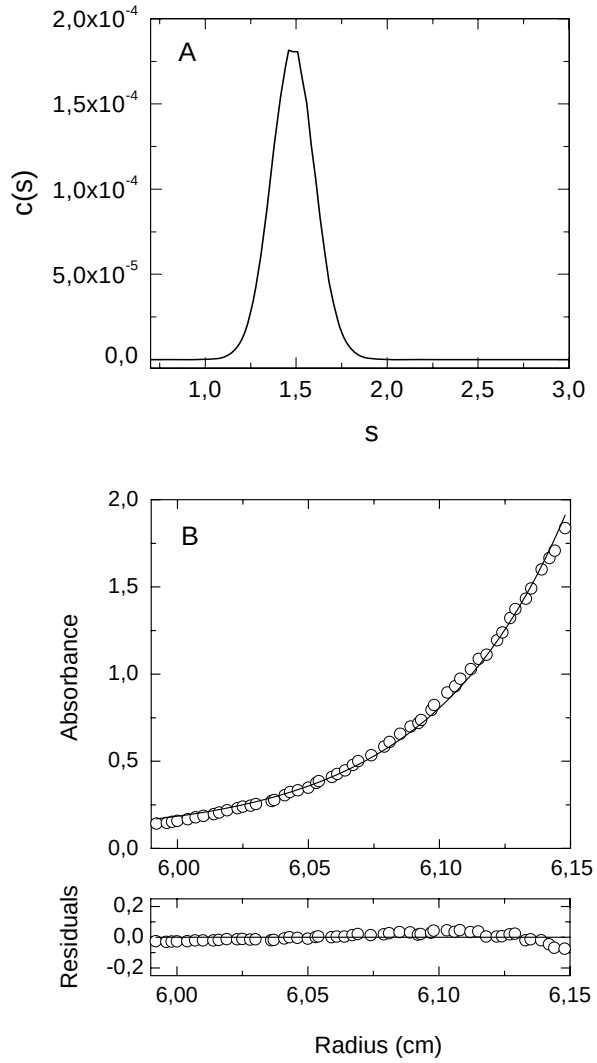

Balsera *et al.* Figure 2

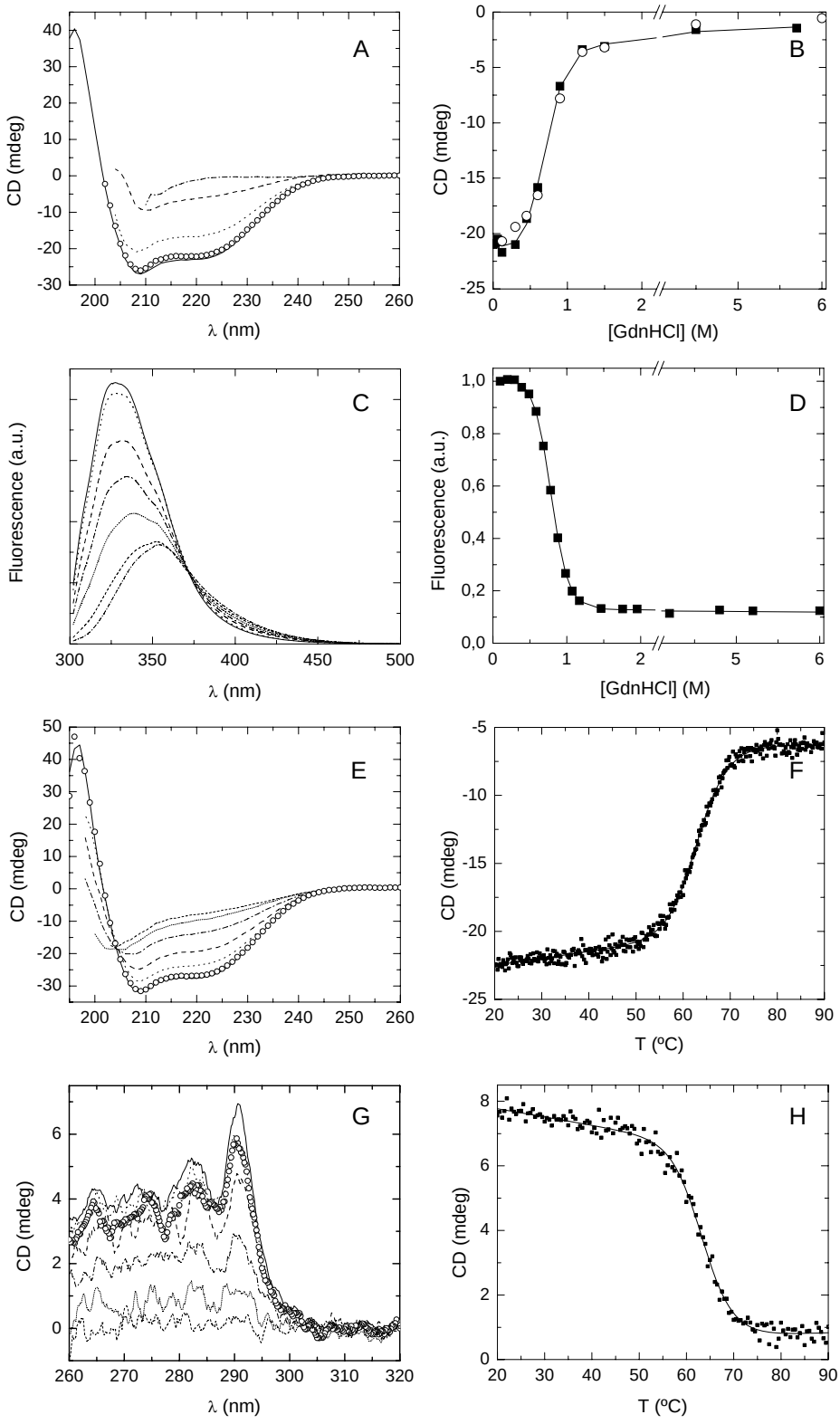

Balsera *et al.* Figure 3

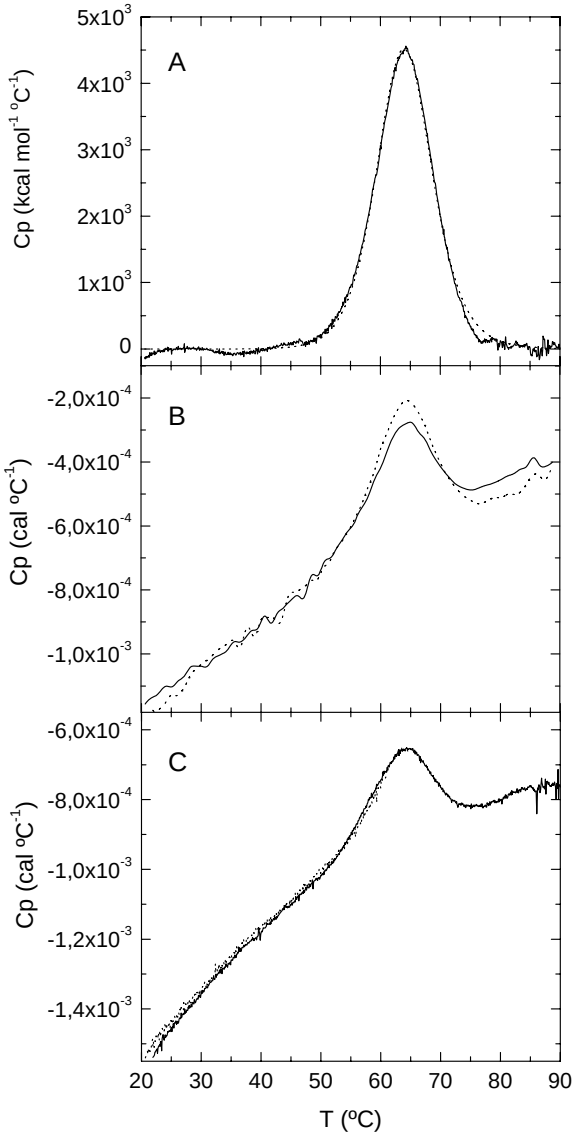

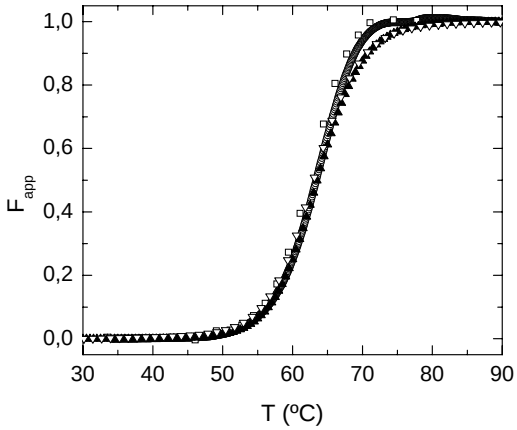
1,0
0,8
0,6
0,4
0,2
0,0
F app
30
40
50
60
70
80
90
T (ºC)

Balsera *et al.* Figure 5